

We are IntechOpen, the world's leading publisher of Open Access books Built by scientists, for scientists

6,900

Open access books available

186,000

International authors and editors

200M

Downloads

Our authors are among the

154

Countries delivered to

TOP 1%

most cited scientists

12.2%

Contributors from top 500 universities



WEB OF SCIENCE™

Selection of our books indexed in the Book Citation Index
in Web of Science™ Core Collection (BKCI)

Interested in publishing with us?
Contact book.department@intechopen.com

Numbers displayed above are based on latest data collected.
For more information visit www.intechopen.com



Hybrid Parallel Robot for the Assembling of ITER

Huapeng Wu, Heikki Handroos and Pekka Pessi
*Lappeenranta University of Technology
 Finland*

1. Introduction

The international thermonuclear experimental reactor (ITER) is a joint international research and development project that aims to demonstrate the scientific and technical feasibility of fusion power. The reactor tokamak (vacuum vessel) is made of stainless steel, and contains nine sectors welded together; each sector has about the size of 10 meter high and 6 meter wide. The sectors of ITER vacuum vessel (VV) (Fig. 1) require more stringent tolerance ($\pm 5\text{mm}$) than normally expected for the size of the structure involved. The walls (inner wall and outer wall) of ITER sectors are of 60mm thick and are joined by high quality leak tight welds. In addition to the initial vacuum vessel assembly, the sectors may have to be replaced for repair. Meanwhile, the machining operations and lifting of a possible e-beam gun column system require extreme stiffness property and good accuracy for a machine tool. The payload to weight ratio also has to be significantly better than it is in the commercial industrial robots.

The conventional robots, providing a high nominal payload, are lack of stiffness and accuracy in such machining condition. Since commercially available machines capable of handling large payloads require floor mounting and their workspaces are insufficient for reaching the cross section at a single mounting position, a special robot is needed. Parallel robots have high stiffness, high dynamic performance and good payload to weight ratio in comparison with the conventional serial robots. Stewart [1] presented the novel idea of six-degree-of-freedom parallel robot in 1960's. A remarkable number of research articles and books about parallel manipulators have been published during the last two decades. There are also a number of successful industrial applications developed [2], [3], [4], [7]. The parallel manipulators have many potential advantages compared with the conventional serial link manipulators. Parallel manipulators are closed-loop mechanism presenting good performances in terms of accuracy, rigidity, high speed, and ability to handle large loads. They are becoming popular in applications such as machining, welding, assembly, flight and vehicle simulators, mining machines, and pointing devices [2], [3], [4], [7]. The most important drawback of parallel robots is the small workspace, which can be made larger by adding additional serial axes in the robot.

For the assembly of the ITER vacuum vessel sector, the precise positioning of welding end-effectors at some distance in a confined space from the available supports will be required,

Source: Parallel Manipulators, Towards New Applications, Book edited by: Huapeng Wu, ISBN 978-3-902613-40-0, pp. 506, April 2008, I-Tech Education and Publishing, Vienna, Austria

while it is not possible using conventional machines or robots. The parallel robot presented in this paper is able to carry out welding and machining processes from inside the ITER vacuum vessel, consisting of a six degree-of-freedom parallel mechanism mounted on a carriage driven by electric motor/gearbox on a rack. The robot carries both welding gun (such as a TIG, hybrid laser or e-beam welding gun to weld the inner and outer walls of the ITER vacuum vessel sectors) and machining tools (to cut and mill the walls with necessary accuracy). It can also carry other heavy tools and parts to a required position inside the vacuum vessel.

The robot offers not only a device but also a methodology for assembling and repairing VV. For assembling, an on-line six-degree-of-freedom-seam-finding algorithm has been developed. The algorithm enables the robot to find welding seam automatically in a very complex environment. For machining, the multi flexible machining processes carried out automatically by the robot have also been investigated, including edge cutting, smoothing, and defect point milling. The kinematic design of the robot has been optimised for the ITER access and a hydraulically actuated prototype has been built. Finally the experimental results are presented and discussed. The earlier development phases of the robot are presented in [8] and [9].

2. Structure of VV and assembling process

The inner and outer walls of the VV of ITER are made of 60mm-thick stainless steel 316L and are welded together through an intermediate, so-called "splice plate", inserted between the sectors to be joined. The splice plates have two important functions: (i) to allow access to bolt together the thermal shield between the VV and coils; and (ii) to compensate the mismatch between adjacent sectors to give a good fit-up of the sector-sector butt weld. The robot's end-effector will have to pass through the inner wall splice plates opening to reach the outer wall. As shown in Fig.1, the assembly and repairing processes have to be carried out from inside the vacuum vessel.

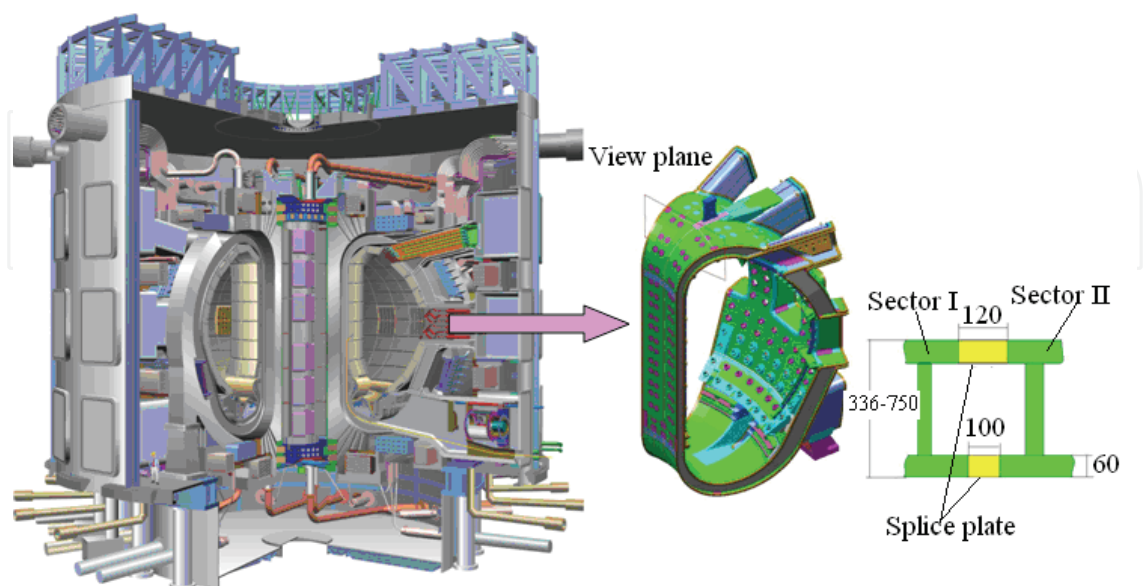


Fig.1 ITER and VV sectors to be welded

The assembly or repair will be performed according to four phases: cutting, edge machining and smoothing, welding, and non-destructive tests (NDT) control. The robot will carry out welding, machining, and inspecting inside the VV. The maximum robot force arises from cutting. It can be up to 3kN.

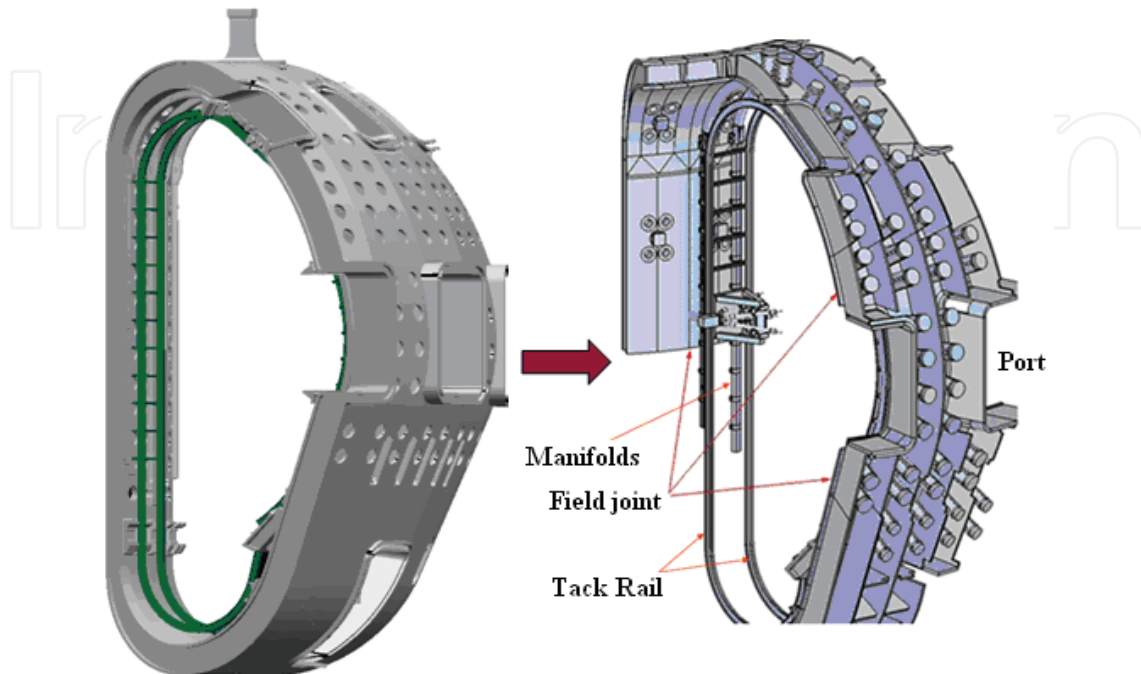


Fig.2 The track rail mounted inside VV and robot on the track

In order that the robot can operate in the cross section of the vessel, a track is assembled inside the sector. The track has a rack on one side of the rail and it is supported by manifolds and beams (shown in Fig. 2). The robot driven on the rail carries out welding or machining along the edge of the sector. After finishing the assembly of two sectors, the robot has to be moved to the next sector where there is also a track assembled. After finishing the assembly of all the sectors, the robot can be taken out via the port of VV.

3. Kinematics of parallel robot

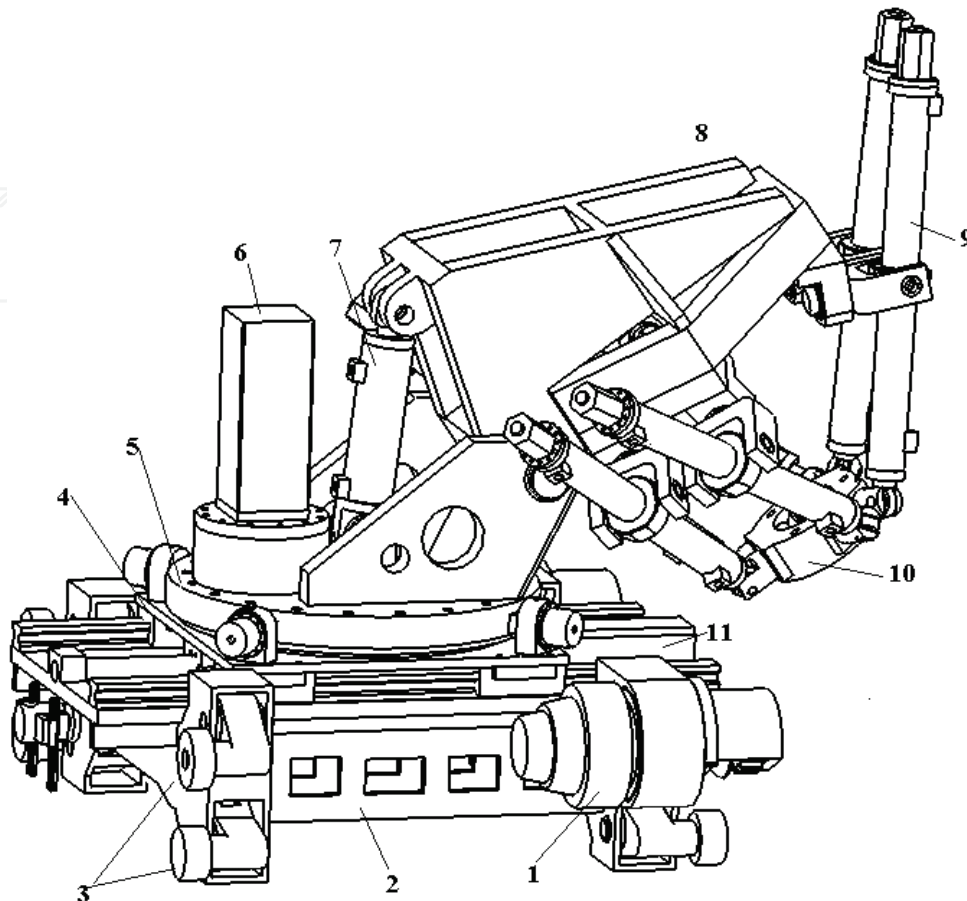
3.1 Structure of parallel robot

The proposed parallel robot has ten degrees of freedom (Fig. 3). It consists of two relatively independent sub-structures: (i) carriage, which provides four additional degrees of freedom, i.e., rotation, linear motion, tilt rotation and tracking motion, and these four degrees are added to enlarge the workspace and to offer high mobility; and (ii) the Hexa-WH parallel mechanism driven by six hydraulic cylinders contributes six degrees of freedom for the end-effector. Thus the robot is a hybrid redundant manipulator with four extra degrees of freedom provided by serial kinematic links.

a). Carriage mechanism

The carriage mainly consists of 5 units. i) *Carriage frame*: The carriage frame is a complex structure welded by multi-steel-plates, and it is able to carry high payload and offers enough room to maintain mechanisms. Stiffness and weight are the most important considerations in the design, and they have been optimized to achieve necessary stiffness

with light weight. *ii) Tracking drive unit:* The tracking drive unit consists of electric motor, reduction unit CYCLO, V-shape bearing, and driving gear. The electric servo motor with



1. Drive motor 2. Carriage frame 3. Compensate mechanisms 4. Linear table
5. Rotation table 6. Rotation drive unit 7. Tip drive cylinder 8. Hexa-WH frame
9. Hexa-WH drive cylinder 10. End effector 11. Linear drive motor

Fig. 3 Parallel robot

position feedback controller offers the high accurate motion. In order to output large torque to drive the heavy mass and payload, the reduction unit CYCLO is added to the motor to reduce speed and to transmit high torque to the driving gear. Two V-shaped wheels keep the carriage on the tracking rail at right position to avoid the cross motion. Two drive units are used in the carriage to offer enough torque in order to drive the robot and payload around inside the VV. *iii) Compensation mechanism:* The compensation system is an important unit that limits the backlash caused by the inaccurate assembling of the tracking rail and compensates the distance changing between the wheels in bending area. As the shape of the VV is very complicated, it is difficult to keep the tracking rails lying on the VV surface in the accurate position. The position tolerance can be up to $\pm 2\text{mm}$. The distance of the coupled wheels has to be adjusted to follow the changes of the rail, and all the wheels must touch the parallel rails with certain force during motion; hence an adaptive distance compensation system is needed and it should be able to undertake the summed weight of the robot and the payload, when the robot is upside down at the top position insider VV. Since the total

payload is very heavy, a hydraulic cylinder is applied to justify the compensation force according to the position where the robot is located. Fig. 4 shows the compensation system, where the upside is the tolerance adaptive mechanism that passively follows the changes of track rail and the downside is the hydraulic distance compensation system that ensures a constant force is applied to the rails. *iv) Linear drive unit:* The linear drive unit enlarges the workspace of the robot, and consists of five parts: ball screw drive unit, servo motor, rails, linear bearings, and a table. Two parallel rails are fixed on the carriage frame to offer the motion crossing the frame and to extend the distance of the robot in direction Y. In direction Y, the distance from the inner board to the outer board can be 900mm in one VV sector, i.e., the robot needs longer reach in this direction, and the linear drive unit helps the robot end-effector to reach the farther border of the VV. *v) Rotation drive unit:* This unit offers a rotation motion about the Z axis, so that the robot can machine the flexible houses on the inner wall at any position. The rotation drive unit consists of slewing bearing, drive gear, reduction unit CYCLO, and servo motor. The slewing bearing integrates bearing and gear together, leading to a compact structure with light weight. The rotation of the unit can reach $\pm 180^\circ$.

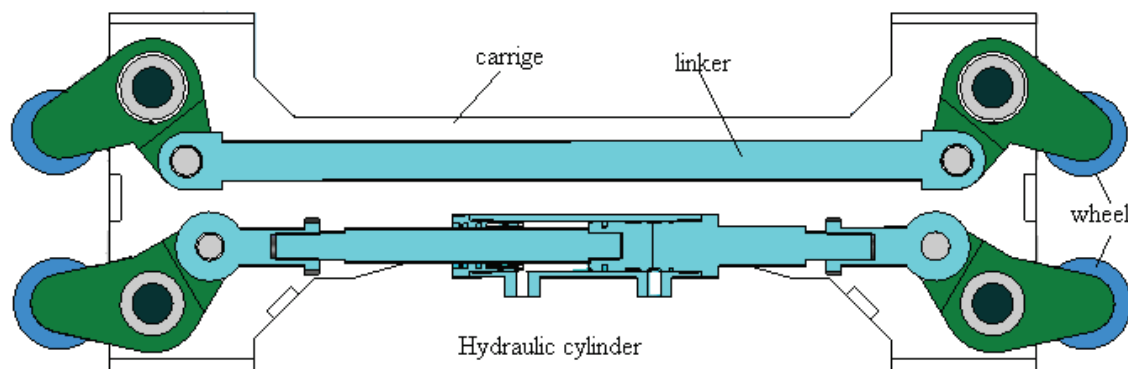


Fig. 4 Compensation mechanism

b). Hexa-WH

A Stewart based mechanism, driven by six servo control water hydraulic cylinders, offers six-degree freedom to the end-effector, where the machining head and welding gun are mounted. Because of the special shape of the VV, a full six-degree freedom motion for tool is needed to enable the robot to carry out welding and machining. The Hexa-WH can offer the required accuracy and the high force capacity due to its novel configuration and the hydraulic drive.

3.2 Kinematics model

The kinematics model is very important for the robot motion control. As the robot has redundant degree freedom, it is difficult to find the kinematics solution directly. The kinematics models can first be set up for the carriage and the Hexa-WH separately, and then be combined together by using an optimization algorithm in solving the redundant problem [4], [5].

a). Forward kinematics

As described above, the carriage offers the robot the four-degree freedom: two linear motions and two rotations; while the Hexa-WH offers the end-effector the full six-degree freedom. The transformation matrix of the robot can be defined as:

$$T_c = T_1 \cdot T_2 \cdot T_3 \cdot T_4 \cdot T_5, \quad (2)$$

where

$$T_1 = \begin{bmatrix} 1 & 0 & 0 & X_1 \\ 0 & 1 & 0 & Y_1 \\ 0 & 0 & 1 & Z_1 \\ 0 & 0 & 0 & 1 \end{bmatrix},$$

$$T_2 = \begin{bmatrix} 1 & 0 & 0 & X_2 \\ 0 & 1 & 0 & Y_2 \\ 0 & 0 & 1 & Z_2 \\ 0 & 0 & 0 & 1 \end{bmatrix},$$

$$T_3 = \begin{bmatrix} c\phi & -s\phi & 0 & X_3 \\ s\phi & c\phi & 0 & Y_3 \\ 0 & 0 & 1 & Z_3 \\ 0 & 0 & 0 & 1 \end{bmatrix},$$

$$T_4 = \begin{bmatrix} 1 & 0 & 0 & X_4 \\ 0 & c\phi & -s\phi & Y_4 \\ 0 & s\phi & c\phi & Z_4 \\ 0 & 0 & 0 & 1 \end{bmatrix},$$

$$T_5 = \begin{bmatrix} cac\beta & cas\beta s\gamma - sac\gamma & cas\beta c\gamma + sas\gamma & X_5 \\ sac\beta & sas\beta s\gamma + cac\gamma & sas\beta c\gamma - cas\gamma & Y_5 \\ -s\beta & c\beta s\gamma & c\beta c\gamma & Z_5 \\ 0 & 0 & 0 & 1 \end{bmatrix}.$$

Once the parameters of joints are given, the forward kinematics of the robot can be defined as

$$\vec{P} = T \cdot \vec{P}_0 = T_1 \cdot T_2 \cdot T_3 \cdot T_4 \cdot T_5 \cdot \vec{P}_0. \quad (2)$$

To solve the forward kinematic model of the Hexa-WH, the numeric iterative method can be employed and it can be solved from its inverse kinematic model given later in the chapter.

b). Inverse kinematic model of robot

As the robot has four-degree freedom of redundancy, we give an inverse kinematic model first to the carriage, then to the Hexa-WH.

Inverse kinematic model of carriage: The inverse kinematic model of the carriage is defined to find the values of the four actuators with respect to the frame \mathcal{o} for a given position and an orientation of P_4 on the Hexa-frame. The principle of the carriage mechanism is shown in Fig. 5. In the application, rotation angle ϕ is fixed only at a few values, 0° , $\pm 90^\circ$, and 180° , and we can calculate the values of other actuators by fixing ϕ , i.e., for a given position $P_4(x, y, z)$, the centre of the Hexa-Frame, we have

$$X + (r_0 + r_1 \cos \phi) \cos \phi = x, \tag{3}$$

$$Y + (r_0 + r_1 \cos \phi) \sin \phi = y, \tag{4}$$

$$r_1 \sin \phi = Z. \tag{5}$$

Then

$$\phi = \arcsin(Z / r_1), \tag{6}$$

$$X = x - (r_0 + r_1 \cos \phi) \cos \phi, \tag{7}$$

$$Y = y - (r_0 + r_1 \cos \phi) \sin \phi. \tag{8}$$

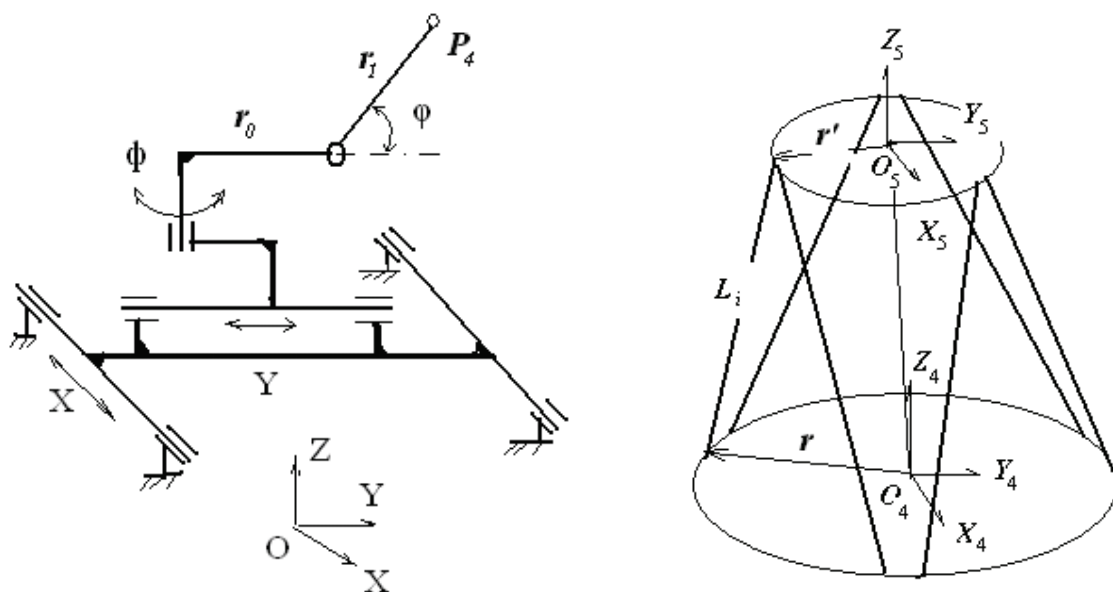


Fig. 5 a) Mechanism of carriage, b) Hexa-WH

Inverse kinematic model of Hexa-WH: The inverse kinematic model for the Hexa-WH is defined to find the values for each cylinder at a given position and an orientation of the end-effector with respect to the Hexa-frame. Here O_4 is coincided with P_4 on the carriage side. Fig.5 b) demonstrates the coordinates of the Hexa-WH.

The inverse kinematics model for the Hexa-WH is

$$\vec{L}_i = \vec{O_4O_5} + R \cdot \vec{r}'_i - \vec{r}_i \quad (i = 1, 2, \dots, 6), \tag{9}$$

where

$$R = \begin{bmatrix} c\alpha c\beta & c\alpha s\beta s\gamma - s\alpha c\gamma & c\alpha s\beta c\gamma + s\alpha s\gamma \\ s\alpha c\beta & s\alpha s\beta s\gamma + c\alpha c\gamma & s\alpha s\beta c\gamma - c\alpha s\gamma \\ -s\beta & c\beta s\gamma & c\beta c\gamma \end{bmatrix},$$

\vec{r}_i denotes the vector of the joint of the i^{th} cylinder on the Hexa-frame with respect to frame \mathbf{o}_4 and \vec{r}'_i is the vector of the joint of the i^{th} cylinder on the end-effector with respect to frame \mathbf{o}_5 .

The length of each cylinder can be found, when $(x, y, z, \gamma, \beta, a)$ is defined with respect to frame \mathbf{o}_4 .

$$l_i = |\vec{L}_i| = \sqrt{(O_4 O_5 + R \cdot \vec{r}'_i - \vec{r}_i) \cdot (O_4 O_5 + R \cdot \vec{r}'_i - \vec{r}_i)}. \quad (10)$$

There are two ways to combine the two inverse kinematic models to get the solution of the whole robot. One simple way is to calculate the coordinates $(x, y, z, \gamma, \beta, \alpha)$ of the end-effector with respect to $\{O_4\}$ and the values for each actuator from equations (3-10) for the given coordinates of the end-effector with respect to frame $\{\mathbf{o}\}$, while fixing $\{O_4\}$ at a certain position with respect to frame $\{\mathbf{o}\}$ according to experience. The another way is to use an optimization algorithm to find redundant solution, which is subjected to minimize the deflection of the robot during motion, i.e., $\min_l f(\bar{q}, \bar{l})$, where f is the deflection model of the robot, \bar{q} is the position vector of the end-effector, and \bar{l} is the value vector of ten actuators. For a given \bar{q} we can find \bar{l} by solving the optimization problem $\min_l f(\bar{q}, \bar{l})$.

4. Control system

4.1 Hydraulic control system

Fig.6 shows the water hydraulic system. Pressure servo control is applied in locking cylinders. Position servo controller is used in cylinders 1-7. There are three loops in the servo position control: the position loop together with the speed loop that provide an accurate and fast trajectory tracking; and the load pressure feedback loop that is applied to damping the self-excited oscillations, which normally occur in the natural frequency. The speed loop can eliminate the speed error, while the pressure feedback damps the vibration of hydraulic actuators (Fig. 7).

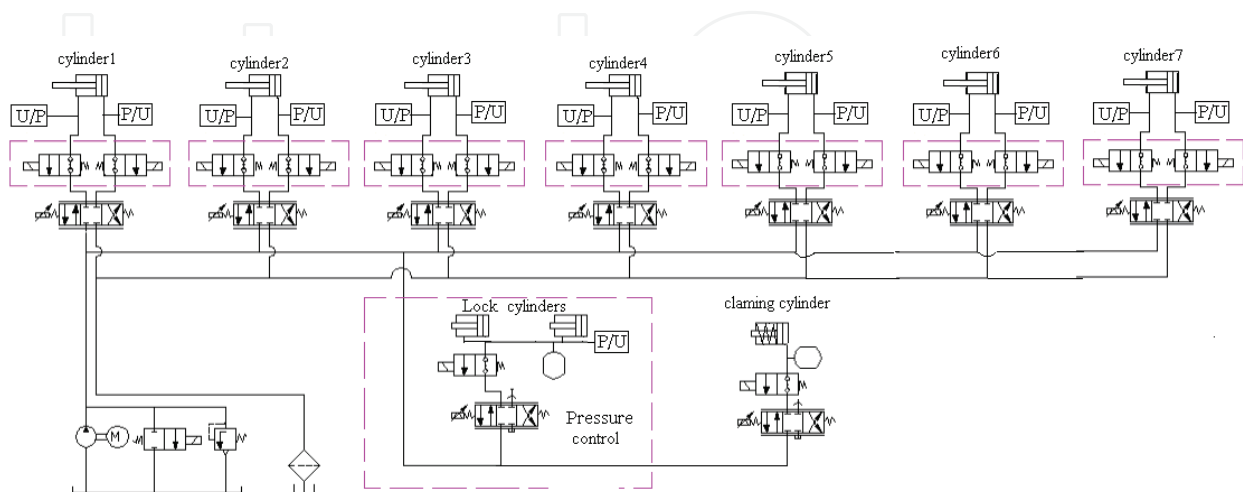


Fig.6 Water hydraulic circle

The hydraulic cylinders normally lack damping that makes the cylinder control difficult by using conventional PID-controllers. The damping can effectively be increased by means of load pressure feedback. The major drawback in using pressure feedback is its negative effect on the static stiffness of the actuator. To overcome this problem, the high pass filters are used in the load pressure feedback loops. The high pass filter removes the negative effect of pressure feedback at low frequency.

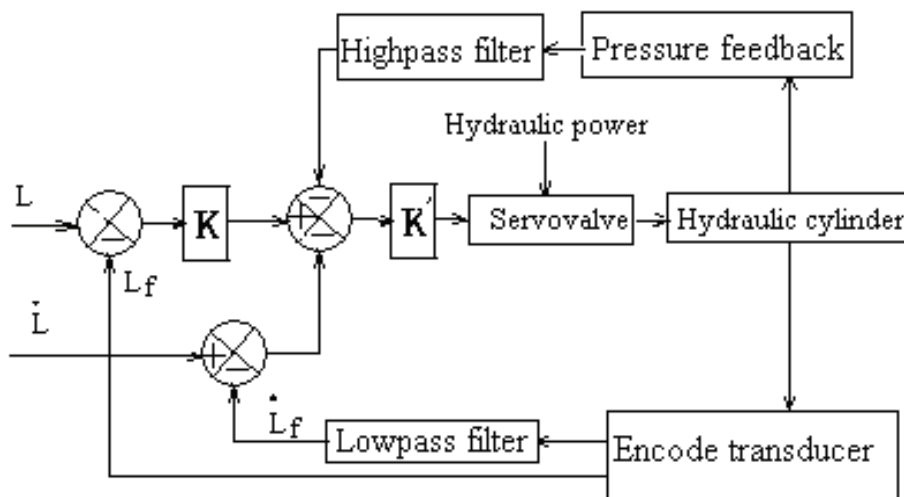


Fig.7 Hydraulic servo position control

4.2 Motor control

Two drive motors contribute effort for the tracking motion of the robot. As the tracking rails are not always straight, the speeds of the two motors are not the same when the robot is moving. The torque control together with a position feedback algorithm is implemented. Fig. 8 shows the control principle.

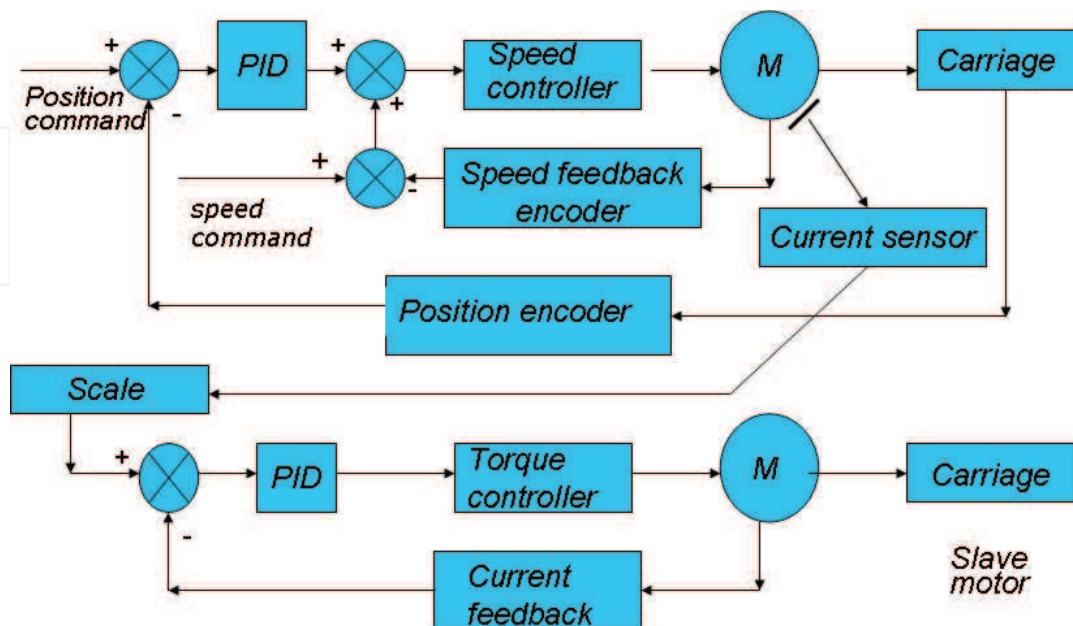


Fig. 8 Tracking motor control

In this method, one motor works as master, and another one works as slave. For the master motor, the position control plus the speed control is applied to guarantee the required speed and position accuracy of the carriage on the tracking rail. For the slave motor, the torque control is applied, which contributes the driving torque for the robot.

4.3 Control of hardware and software

Because there are no commercial controller and software available for the special functions of the parallel robot, an open architecture of hardware and programmable software are being developed. Fig. 9 shows the structure of hardware control system. The controller is an industrial-PC-based motion controller. It provides a reliable and easy-at-use environment for controlling the robot because Earthnet bus is used in the connection of iPC and I/O interfaces.

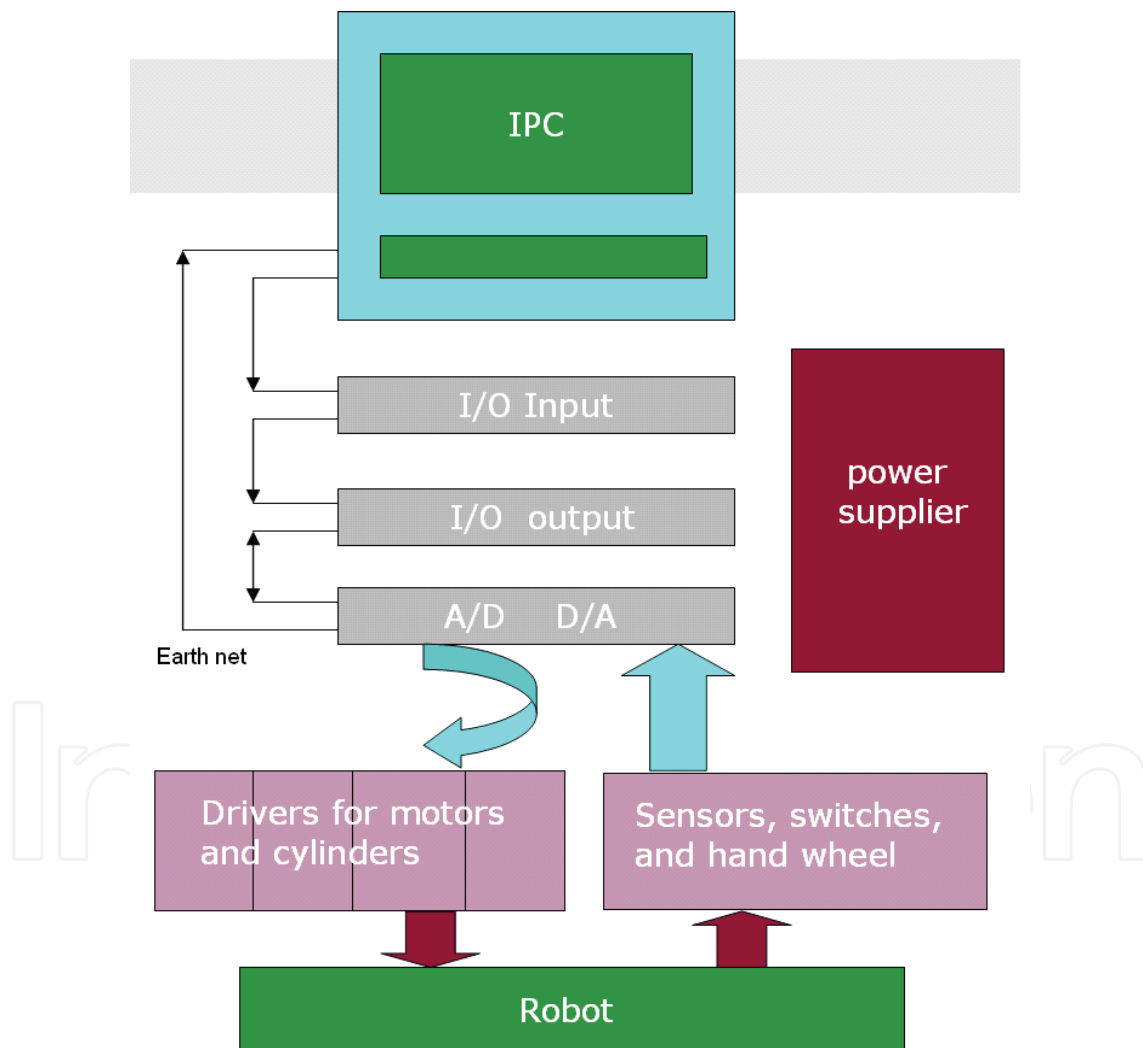


Fig.9 Structure of robot controller

The software is defined in Fig.10, including graphical interface, trajectory planning, forward and inverse kinematics models, interpolator, controller, and I/O interface functions. And

those functions have to be integrated with the program offered by iPC and run completely in real time.

Graphical interface is a high level program, it includes parameter setting, condition monitoring, and graphical visualization functions. User can easily exchange information with this program.

Trajectory planning is also a high level program. As the robot has redundant actuators, the trajectory planning is much more difficult than usual, so an optimization algorithm, which is subjected to minimize the deflection of the robot during motion, has been employed.

Forward and inverse kinematics models and interpolator are real time functions, which generate data for motion controller.

Controller is a real time function including water hydraulic controller and motor controller. As the robot has two tracking motors and the speed of the motors are not always the same at some positions, a master-slave control algorithm has been used.

I/O interface functions are real time functions, which enable transferring data from sensor to controller and from controller to driver.

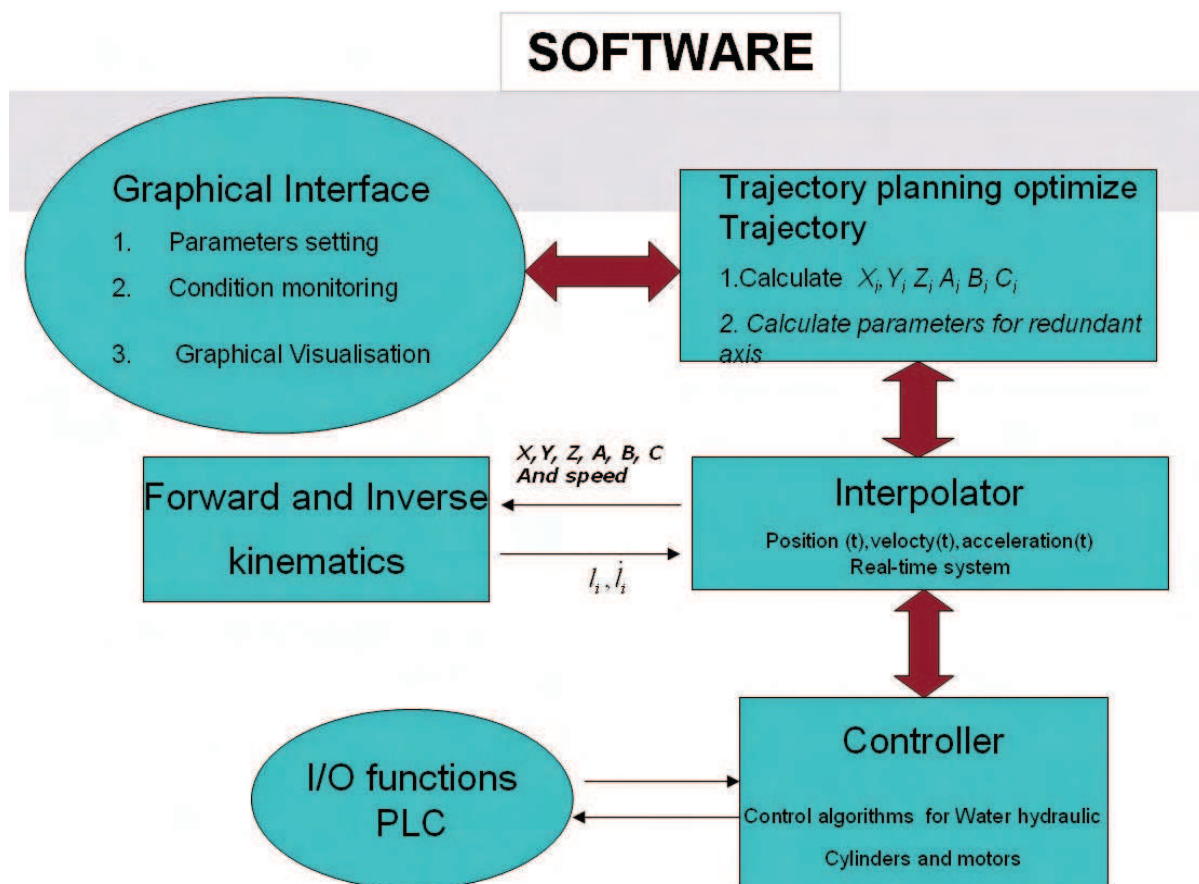


Fig. 10 Structure of software

5. Machining and welding testing mock-up

The parallel robot has been built in Lappeenranta University of Technology and the machining and welding test mock-up is designed shown in Fig.11. The mock-up is one

quarter of a sector built up for testing the machining and welding functions of the robot. Before the mock-up, some welding and machining tests have been carried out with the first prototype of the parallel robot named Penta-WH. The laser welding with seam tracker has been tested in stainless steel and the machine cutting with disc saw has been tested in the stainless steel machining process. The robot performs well in the tests.

5.1 Machining

The cutting test was carried out with stainless steel. The high speed steel cutting tool was used in the test. It is 200mm in diameter and 4mm in thickness. The problem in the experiment was that the high speed cutting tool wore out quickly during the cutting. The carbide tools, which are much more suitable for cutting stainless steel, are suggested to be used in the cutting operations in the ITER.

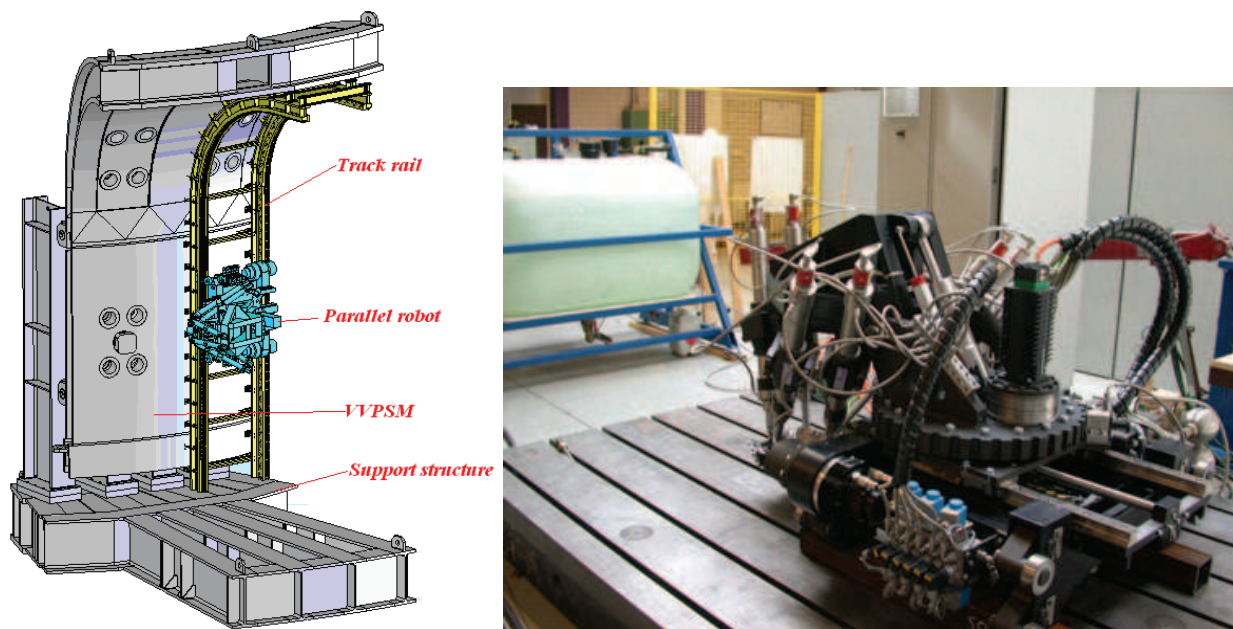


Fig.11 VVPSM mock-up and final version of parallel robot

5.2 Laser welding test

In the ITER assembly, the high quality welds are required to avoid the leak of tritium. They can be achieved by a highly automatic and remotely controlled welding procedure. To guarantee the welding quality, a seam tracker, which guides the robot motions along the center of a welding seam, is employed. With a seam tracker, the parallel robot has the capability to correct the motion trajectory on-line to keep the welding head at the right position and orientation in relation to the welding seam. The position errors of the welding head related to the welding seam caused by the distortion of material and the imprecise track rail are described in Fig.12.

During testing, the laser welding head is mounted on the end-effector of the parallel robot while the seam tracking sensor is mounted in the front of the welding head for guiding the robot welding (Fig.12). The work piece is assembled randomly in the y and z directions during testing. It has approximately a one-degree angle about the Y and Z-axes. The position of seam is unknown for the robot before the seam finding. The maximum output power used in the testing is 3 kW YAG. It has a 200mm focal length resulting in a 0.6 mm diameter focal spot on the work piece. The beam parameter product is 25 mm-mrad. The work piece is made of stainless steel AISI 316LN. It has a 7mm-thickness, 600mm-length, and 0.2mm-root gap for welding.

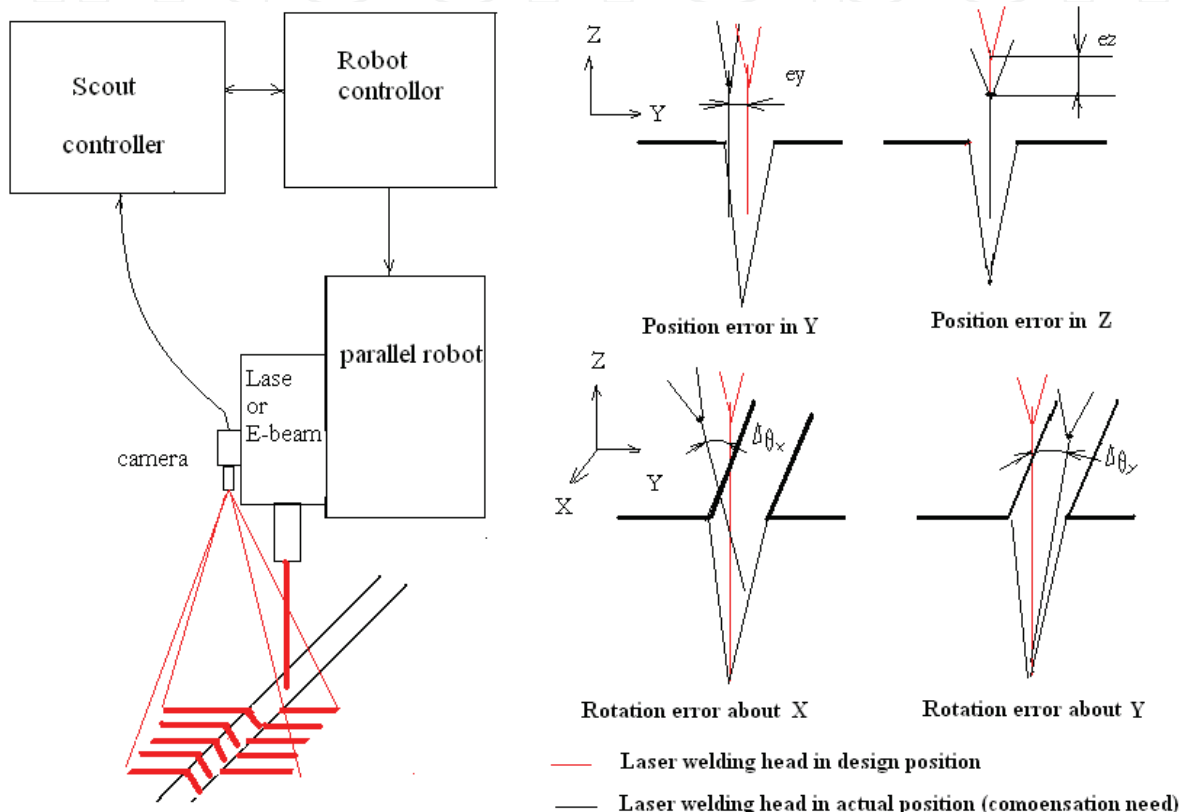


Fig.12 Principle of seam tracker

Two seam tracking algorithms were tested during laser welding trials. One is the off-line teaching algorithm that has two steps: (i) the robot follows the planned trajectory of the seam and records the data from the seam tracker; and after that (ii) the robot compensates the motion trajectory from the data recorded and starts welding following the new motion trajectory. Fig.13 shows the welding results. The second algorithm is the on-line teaching algorithm. In the algorithm, the robot corrects the trajectory on-line using data from the seam tracker during the welding motion. Fig.14 shows the welding results achieved during the tests. From the test results, we can conclude that the on-line teaching algorithm is better than the off-line teaching algorithm, because the on-line teaching algorithm compensates the distortion of the work piece during the welding process.

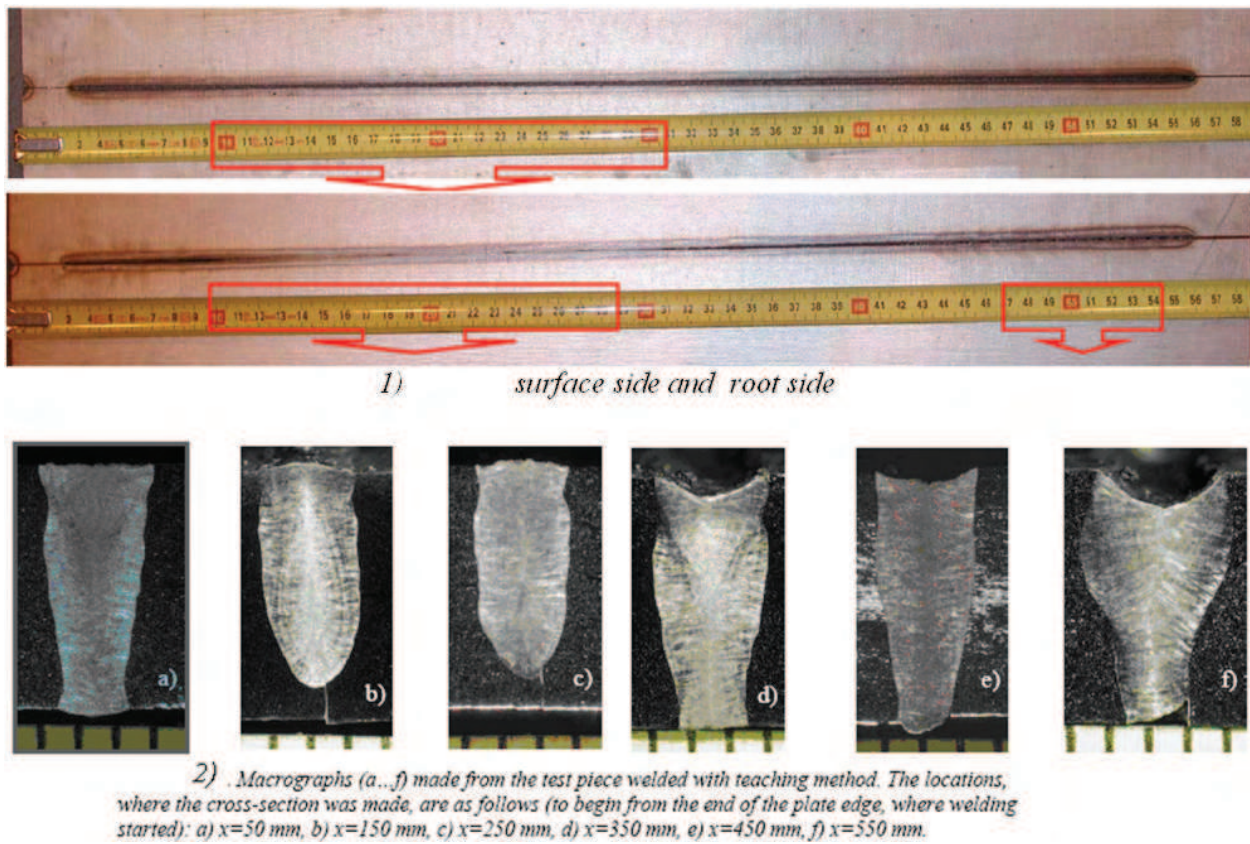


Fig.13 Off-line teaching welding results

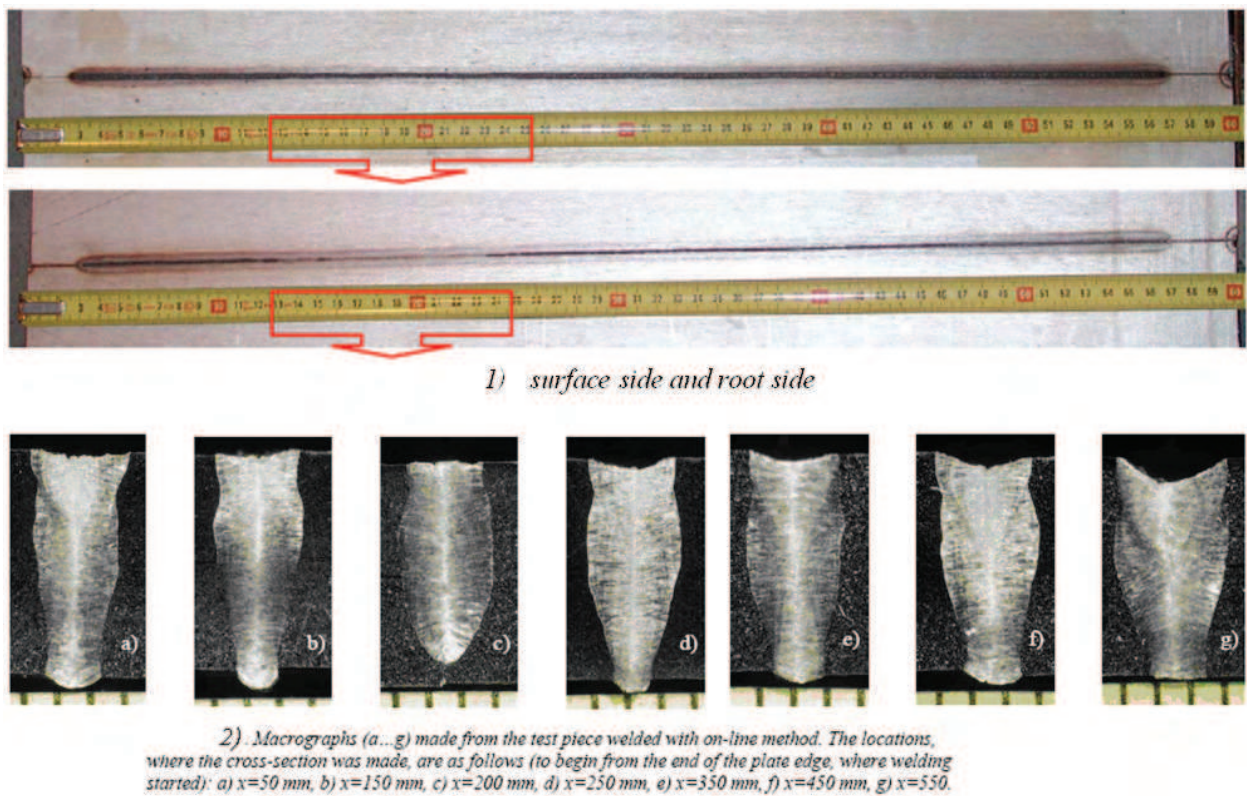


Fig.14 On-line tracking welding results

6. Conclusion

A hybrid parallel robot with four additional serial motion axes is developed for carrying out the necessary machining and welding tasks in the assembling and repairing of the ITER Vacuum Vessel. The robot is capable of holding all necessary machining tools and welding end-effectors in all positions accurately and stably. The kinematics analysis of the robot is presented. The models are complex because of the redundant structure of the robot. The models are separately derived for the Hexa-WH and the carriage mechanism. An optimization algorithm finds the solution in the trajectory planning, ensuring the maximum stiffness during the robot motion. The experiments of the laser welding tests with the seam tracker have been carried out. Both the on-line and off-line teaching algorithms have been developed and the results show that the online teaching algorithm is better. The machining cutting tests with stainless steel have been tested. The entire design and testing process of the robot is a very complex task due to the high specialization of the manufacturing technology needed in the ITER reactor. The results demonstrate the applicability of the proposed solutions quite well.

7. Acknowledgement

The laser welding test is carried out in collaboration with the laser laboratory of VTT in Lappeenranta, Finland, the whole work, supported by the European communities under the contract of Association between EURATOM/Finnish TEKES, was carried out within the framework of the European Fusion Development Agreement, and the views and opinions expressed herein do not necessarily reflect those of the European Commission.

8. References

- D. Stewart (1965), A platform with six degree of freedom, *Proc. Inst. Mech. Eng.*, London, Vol. 180, pp. 371-386.
- T. C. Arai, K. Homma, H. Adachi, and Nakamura (1991), Development of parallel link manipulator for underground excavation task, *Proc. Int. Symposium on Advanced Robot Technology*, pp. 541-548.
- C. Gosselin and J. Hamel (1994), The agile eye: A high-performance three degree of freedom camera -orienting device, *Proc. IEEE Int. Conference on Robotics and Automation*, pp. 781-786.
- L. W. Tsai (1999), *Robot analysis: The mechanics of serial and parallel manipulators*, A Wiley-Interscience Publication, John Wiley & Sons Inc.
- G. Lebreton, K. Liu, and L. Lewis (1993), Dynamic analysis and control of a Stewart platform manipulator, *J. Robotic Systems*, Vol. 5, No. 10, pp. 629-655.
- G. Zheng, L. S. Haynes, J. D. Lee and R. Carroll (1992), On the dynamic model and kinematic analysis of a class of Stewart platforms, *Robotics and Autonomous Systems*, Vol. 9, pp. 237- 254.
- K. H. Häfele, H. Haffner, and P. Spencer (1992), "Automatic Fetting Cell- An Example for Applying Computer- Aided Robotics", *Industrial Robot*. Vol.19 No. 5. pp.31-34

- H.Wu, H. Handroos, P. Pessi, J. Kilkki, L. Jones (2005), "Development and control towards a parallel water hydraulic weld/cut robot for machining processes in ITER vacuum vessel", Fusion Engineering and Design.
- H. Wu, H. Handroos (2006), Mechatronics design and development towards a heavy-duty waterhydraulic welding/cutting robot in Book: Mechatronics for Safety, Security and Dependability in a New Era. Elsevier.

IntechOpen

IntechOpen



Parallel Manipulators, towards New Applications

Edited by Huapeng Wu

ISBN 978-3-902613-40-0

Hard cover, 506 pages

Publisher I-Tech Education and Publishing

Published online 01, April, 2008

Published in print edition April, 2008

In recent years, parallel kinematics mechanisms have attracted a lot of attention from the academic and industrial communities due to potential applications not only as robot manipulators but also as machine tools. Generally, the criteria used to compare the performance of traditional serial robots and parallel robots are the workspace, the ratio between the payload and the robot mass, accuracy, and dynamic behaviour. In addition to the reduced coupling effect between joints, parallel robots bring the benefits of much higher payload-robot mass ratios, superior accuracy and greater stiffness; qualities which lead to better dynamic performance. The main drawback with parallel robots is the relatively small workspace. A great deal of research on parallel robots has been carried out worldwide, and a large number of parallel mechanism systems have been built for various applications, such as remote handling, machine tools, medical robots, simulators, micro-robots, and humanoid robots. This book opens a window to exceptional research and development work on parallel mechanisms contributed by authors from around the world. Through this window the reader can get a good view of current parallel robot research and applications.

How to reference

In order to correctly reference this scholarly work, feel free to copy and paste the following:

Huapeng Wu, Heikki Handroos and Pekka Pessi (2008). Hybrid Parallel Robot for the Assembling of ITER, Parallel Manipulators, towards New Applications, Huapeng Wu (Ed.), ISBN: 978-3-902613-40-0, InTech, Available from:

http://www.intechopen.com/books/parallel_manipulators_towards_new_applications/hybrid_parallel_robot_for_the_assembling_of_iter

INTECH
open science | open minds

InTech Europe

University Campus STeP Ri
Slavka Krautzeka 83/A
51000 Rijeka, Croatia
Phone: +385 (51) 770 447
Fax: +385 (51) 686 166
www.intechopen.com

InTech China

Unit 405, Office Block, Hotel Equatorial Shanghai
No.65, Yan An Road (West), Shanghai, 200040, China
中国上海市延安西路65号上海国际贵都大饭店办公楼405单元
Phone: +86-21-62489820
Fax: +86-21-62489821

© 2008 The Author(s). Licensee IntechOpen. This chapter is distributed under the terms of the [Creative Commons Attribution-NonCommercial-ShareAlike-3.0 License](#), which permits use, distribution and reproduction for non-commercial purposes, provided the original is properly cited and derivative works building on this content are distributed under the same license.

IntechOpen

IntechOpen